Vol. 24, No. 1(2025) IA25426
Revista Mexicana de Ingeniería Química

Potential use of artichoke (*Cynara cardunculus* L.) waste packed in filter bags for the removal of hexavalent chromium from water

Uso potencial de residuos de alcachofa (*Cynara cardunculus* L.) empaquetados en bolsas filtrantes para la eliminación de cromo hexavalente presente en agua

K.F. Diaz-Rodriguez*, B. M. Salazar-Pinto, S. S. Flores-Calla, E. G. Gonzales-Condori*
Universidad Tecnológica del Perú (UTP), Av. Tacna y Arica 160, Arequipa, Perú.
Received: September 28, 2024; Accepted: February 14, 2025

Abstract

The objective of the study was to evaluate the removal of Cr (VI) from water using artichoke (*Cynara cardunculus* L.) waste powder packed in filter bags. For this purpose, the effects of the initial Cr (VI) concentration and adsorbent dosage factors were first evaluated using a $3^2 \times 3$ factorial design. Subsequently, the effect of pH, time, and temperature on the removal process was evaluated. The results show that a dosage of 5 g/L and pH=2 would achieve a higher adsorption efficiency. FTIR analysis showed the presence of functional groups such as hydroxyl, carbonyl, hydrocarbon chains, and aromatic groups characteristic of lignocellulosic compounds, which would be related to the adsorption process. The morphology of the artichoke evaluated by SEM indicates an irregular surface characteristic of adsorbents. The kinetic model that best describes the adsorption process corresponds to the pseudo-second order model. The Langmuir model that best fits the experimental data indicates that the adsorption process occurs in a monolayer with a maximum adsorption capacity of 7.89 mg/g. The mechanisms involved in adsorption correspond to electrostatic attraction and chemical adsorption. With these findings, it is concluded that artichoke waste packed in filter bags for the removal of Cr (VI) in water has proven to be an effective, simple, low cost and environmentally friendly process.
Keywords: Cynara cardunculus, artichoke, Cr (VI), adsorption, water.

Resumen

El objetivo del estudio fue evaluar la remoción de Cr (VI) de agua empleando polvo de desechos de alcachofa (*Cynara cardunculus* L.) empaquetados en bolsas filtrantes. Para esto, primero se evaluaron los efectos de los factores de concentración inicial de Cr (VI) y dosis de adsorbente mediante un diseño factorial $3^2 \times 3$. Posteriormente, se evaluó el efecto del pH, el tiempo y la temperatura en el proceso de remoción. Los resultados muestran que una dosis de 5 g/L y un pH=2 lograrían una mayor eficiencia de adsorción. Los análisis por FTIR evidenció presencia de grupos funcionales como hidroxilo, carbonilo, cadenas hidrocarbonadas y grupos aromáticos característicos de los compuestos lignocelulósicos que estarían relacionados con el proceso de adsorción. La morfología de la alcachofa evaluada por SEM indica una superficie irregular característica de los adsorbentes. El modelo cinético que describe mejor el proceso de adsorción corresponde al modelo de pseudo-segundo orden. El modelo de Langmuir que presento mejor ajuste a los datos experimentales indica que, el proceso de adsorción se da en monocapa siendo la capacidad máxima de adsorción de 7.89 mg/g. Los mecanismos involucrados en la adsorción corresponden a una atracción electrostática y la adsorción química. Con estos hallazgos, se concluye que los residuos de alcachofa empaquetadas en bolsas filtrantes para la remoción de Cr (VI) en agua ha demostrado ser un proceso efectivo, simple, de bajo coste y respetuoso con el medio ambiente.
Palabras clave: Cynara cardunculus, alcachofa, Cr (VI), adsorción, agua.

* *Corresponding authors. E-mail*: kfdr2149@gmail.com(KFDR); elvgonzalesc@gmail.com (EGGC);
https://doi.org/10.24275/rmiq/IA25426
ISSN:1665-2738, *issn-e*: 2395-8472

1 Introduction

The tanning industry uses a large amount of water resources, mainly in the soaking, descaling, and neutralizing stages, resulting in an effluent with a high load of organic matter, fats, and heavy metals such as chromium (Cr), outside the maximum permissible limits (MPL) (Fouda *et al*., 2021). Current leather production uses less than 70 % of the Cr applied, turning the surplus into waste (Hossain *et al*., 2017). The most stable states of Cr in water are the trivalent and hexavalent forms (Cr (III) and Cr (VI)), however, Cr (VI) ions are the most lethal and harmful to humans and the environment (Rambabu *et al*., 2020), even at low concentrations (Ali *et al*., 2019). Significant quantities of this metal are discharged into water assets without adequate treatment (Dobrowolski *et al*., 2019). These pollutants in waterways pose a serious threat to the environment (Que *et al*., 2019), being toxic to aquatic ecosystems, soil, and subsoil (Sun *et al*., 2019). In addition, they cause serious health problems in humans, cardiovascular diseases, autoimmune diseases, oxidative stress, cancer, developmental delay, and kidney damage (Arshad *et al*., 2019; Zhang *et al*., 2021).

Removal of toxic metals by adsorption is accepted as a suitable alternative technology (Arief *et al*., 2008). This is a process of transferring metal ions from the liquid phase to the surface of a solid (sorbent), binding by chemical and/or physical interactions (Zhao *et al*., 2016). For this to happen, there must be an affinity between the functional groups of the contaminant and the biomass since the former must be attracted to the latter and bonded by different mechanisms, the phenomenon can occur by ion exchange, precipitation, complexation, or electrostatic attraction (Elgarahy *et al*., 2021). However, if the adsorbed molecule is not fixed at a specific location on the surface, but rather is free to move within the interface, the adsorption is said to be due to Van der Waals forces also called physisorption. Incidentally, if the adsorbate forms strong bonds located at the active centers of the adsorbent, the adsorption can be said to be chemical. Becoming an environmentally friendly (Rosique *et al*., 2016), simple, feasible, low-cost, fast adsorption kinetic process (Petrella *et al., 2018)*. As for the removal efficiency, it will depend on the adsorbent and its capacity to retain metal ions, a technique widely studied using agricultural wastes, maintaining a circular economy.

Artichoke (*Cynara scolymus* L.), is a vegetable mainly intended for industrial consumption and processing (Zuorro *et al*., 2016), with Italy is the world's largest producer of artichoke, with an annual production of more than 400 000 tons (t), followed by Egypt, Spain, and Peru (922 142 t/year) (FAO, 2018), consuming only 30 % as food and eliminating 70 % of the total plant biomass (de Diego-Díaz *et al*., 2021; Lattanzio *et al*., 2009). Artichoke waste consists mainly of the external parts of the flowers, commonly known as bracts, and stems, considered as lignocellulosic substrates, not suitable for human consumption, and generally disposed of as solid waste (de Diego-Díaz *et al*., 2021).

Artichoke waste is a biomaterial with the capacity to remove different contaminants in aqueous solutions, as it can remove drugs such as piroxicam (Samghouli *et al*., 2022) and ketoprofen (Khalfaoui *et al*., 2024), likewise, its capacity to remove dyes such as methylene blue (Bencheikh *et al*., 2020), Bengal Rose (Khalfaoui *et al*., 2022), violet crystal, and congo red was evidenced (Hajji Nabih *et al*., 2023), on the other hand, it has been reported that it can remove heavy metals such as Cu (II) (Bencheikh *et al*., 2021) and Pb (II) (Ergüvenerler *et al*., 2020) in monometallic aqueous solutions and Pb (II), Cd (II), and Cu (II) in multimetallic aqueous solutions (Saavedra *et al*., 2019). This adsorption capacity would be due to chemisorption processes by the presence of alcoholic, carboxylic, sulfonic, and amino groups (Fernández-López et al., 2019).

Therefore, the objective of this work was to evaluate the potential of artichoke residues packed in filter bags as an adsorbent for the removal of Cr (VI). For this purpose, 1) a 3^2x3 experimental design was used to evaluate the effect of the dosage of artichoke waste powder and initial concentration of Cr (VI) on the removal percentage, then 2) the effect of pH on the Cr (VI) adsorption process was evaluated, subsequently, 3) the kinetics and adsorption isotherms were studied, also, 4) the intraparticle diffusion model and the thermodynamic parameters of adsorption were evaluated, and finally, 5) characterizations of the artichoke waste powder were performed by FTIR (Fourier Transform Infrared Spectroscopy) and Scanning Electron Microscopy (SEM).

2 Materials and methods

2.1 *Reagents and Cr (VI) determination*

All reactive grade chemicals are commercially available from Merck. A 1000 mg/L Cr (VI) stock solution was prepared using potassium dichromate ($K_2Cr_2O_7$) and ultrapure water. Hydrochloric acid solutions 0.1 M HCl and 0.1 M NaOH were used to adjust the pH. Additionally, for the spectrophotometric quantification of Cr (VI), solutions of 1 M HCl, acetone, and 1,5-diphenicarbazide were used. For Cr (VI) quantification, a calibration graph was prepared with six concentrations of Cr (VI) using $K_2Cr_2O_7$ in the range of 0.2 to 1.2 mg/L.

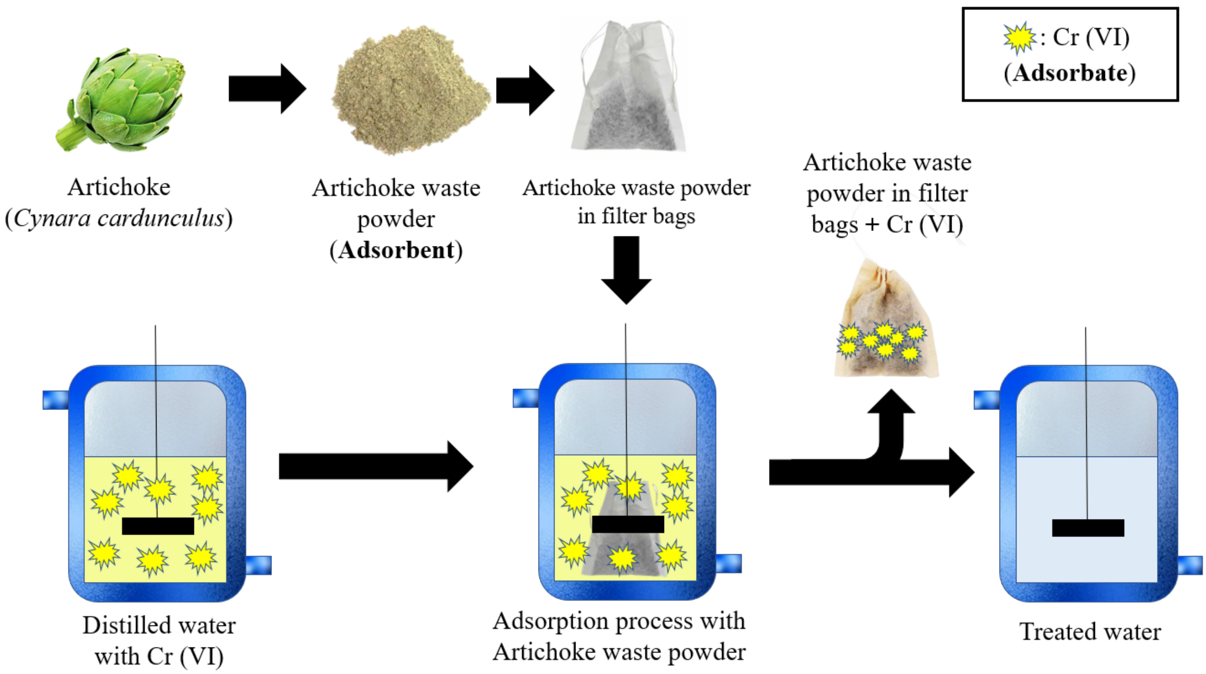

Figure 1. Cr (VI) adsorption process using artichoke waste packaged in filter bags.

A linear equation of y= 0.2783x-0.0042 was obtained. A coefficient of determination R^2=0.9998 was also obtained. This indicates that the method is linear since the R^2 is greater than 0.995 (Quattrocchi *et al*., 1992). The limits of detection and quantification were 0.008 and 0.042 mg/L, respectively.

2.2 *Preparation of adsorbent (artichoke)*

The artichoke waste consisted of waste from an artichoke production company located in the city of Arequipa, Peru. The artichoke waste was washed repeatedly with abundant distilled water, then the bracts and outer stems were cut and dried at 70 °C for 24 h. The artichoke was then washed repeatedly with abundant distilled water (Fernández-López *et al*., 2019). The dried residue was pulverized in a knife mill and then passed through a 40-mesh screen. Subsequently, the artichoke waste powder (AWP) was stored in Kraft paper inside a desiccator to prevent it from capturing moisture.

2.3 *Cr (VI) removal process*

Figure 1 shows the schematization of the Cr (VI) removal process, which consisted of packing determined dosages of AWP in g/L in filter bags to remove the adsorbent more easily from the water and avoid subsequent processes such as filtration or centrifugation. This facilitates the quantification of Cr (VI) by spectrophotometry making the process faster. Once the AWP is packed in the tea bags, they are closed and transferred to jacketed beakers containing Cr (VI) solutions determined at pH adjusted, and the Batch system is agitated at 150 rpm at controlled temperature.

2.4 *Experimental design*

A 3^2x3 factorial design was used, giving a total of 27 experiments taking into account the factors of AWP dosage and initial Cr (VI) concentration. The design factors and levels are presented in Table 1. The agitation time was 30 min, at pH=3 and a temperature of 20 °C. At the end, the AWP filter tea bag was removed and Cr (VI) concentration was quantified using the diphenylcarbazide method using a Thermo Scientific™ Genesys 150 UV/vis spectrophotometer at 540 nm. The concentrations were calculated and then the removal efficiency of each experiment was calculated by calculating the percentage of removal using Equation 1.

$$\%R = \frac{C_0 - C_f}{C_0} \times 100 \tag{1}$$

Where "C_0" and "C_f" correspond to the initial and final Cr (VI) concentration in mg/L, respectively.

Once the calculations were made, the data were taken to the Statgraphics Centurion software where the removal efficiencies obtained in each experiment were analyzed to evaluate the effect of the factors studied in the process using the analysis of variance (p-values <0.05 indicate a significant effect). Finally, using the same software, the removal process was optimized with the main criterion of maximizing the removal percentage.

Table 1. Factors and levels used in the 3^2 x 3 factorial design.

Factor	Level -1	Level 0	Level +1
A: Dosage of artichoke waste powder (g/L)	5	10	15
B: Initial concentration of Cr (VI) (mg/L)	10	30	50

2.5 *Effect of pH*

To determine the effect of pH on the adsorption process, additional experiments were performed in triplicate after optimization. With the values of the optimal factors of AWP adsorbent dosage and initial Cr (VI) concentration, the removal percentages obtained in triplicate at pH=2, pH=3 and pH=4 were compared. Finally, the removal percentages were compared using a one-way analysis of variance and Tukey's *post hoc* test for multiple comparisons. The significance level was 95 % and a p-value<0.05 was considered as a significant difference.

2.6 *Point of Zero Charge*

The AWP charge was determined by the point of zero charge analysis (pH_{PZC}) using the procedure developed by (Worku *et al*., 2023) with some modifications. The process consisted of weighing 1 g of AWP and then taking it to 250 mL flasks where 50 mL of 0.1 M NaCl solution was previously added in Erlenmeyer flasks with the pH adjusted with 0.1 M HCl and 0.1 M NaOH solutions in the pH range of 2 to 12, then agitation was started at 150 rpm for 24 hours. Subsequently, the final pH was calculated. Finally, the pH_{PZC} value was determined from the intersection between the graph of initial vs ΔpH (pH_{final} – initial) and the *x*-axis (Gonzales-Condori *et al*., 2023).

2.7 *Kinetics*

The kinetic study was carried out to evaluate the effect of time on the removal process. For this purpose, adsorption experiments were carried out at 20 °C using optimal Cr (VI) dosage and initial concentration values determined in the factorial design and at the pH at which the highest removal efficiency is achieved. The experiments consisted of taking appropriate samples at 2, 5, 10, 20, 30, 60, 90, 120, 150, and 180 min. Cr (VI) concentrations were quantified in each sample. With the data obtained, the removal kinetics were evaluated using the pseudo-first order and pseudo-second order nonlinear kinetic models using equations 2 and 3, respectively.

$$q_t = q_e(1 - e^{-k_1 t}) \tag{2}$$

$$q_t = \frac{k_2 q_e^2 t}{1 + k_2 q_e t} \tag{3}$$

Where "k_1" (min^{-1}) and "k_2" (g $mg^{-1}min^{-1}$) correspond to the pseudo-first-order and pseudo-second-order constants respectively, "q_e" corresponds to the adsorption capacity in the equilibrium in mg/g at a time "t" (Yang *et al*., 2020). The calculation of these parameters was performed by plotting t vs q_t. "q_t" (mg/g) corresponds to the amount of mg of Cr (VI) in mg adsorbed on 1 gram of adsorbent which was calculated using equation 4.

$$q_t = \frac{C_0 - C_f}{m} \times V \tag{4}$$

Where "m" corresponds to the weight in grams of the adsorbent and "V" is the volume in liters of Cr (VI) solution (Choquenaira-Quispe *et al*., 2024).

The intraparticle diffusion model presented in Equation 5 was also evaluated.

$$q_t = K_{id}^{1/2}(t) + C \tag{5}$$

Where "K_{id}" ($mg \cdot g^{-1} \cdot min^{1/2}$) is the intraparticle diffusion rate constant (Wang *et al*., 2025), and "C" is the model constant associated with the thickness of the boundary layer (Xu *et al*., 2019).

2.8 *Isotherms*

Adsorption isotherms express the surface properties and affinity of the adsorbent. In this study, adsorption isotherms were performed at 20 °C, 30 °C, and 40 °C at optimum conditions. The mathematical models of Langmuir and Freundlich's isotherms presented in equations 6 and 7 respectively were used (Salazar-Pinto *et al*., 2021).

$$q_e = \frac{q_m K_L C_e}{1 + K_L C_e} \tag{6}$$

$$q_e = K_f C_e^{1/n} \tag{7}$$

Where "q_e" (mg/g) and "C_e" (mg/L) correspond to the adsorption capacity shown by the adsorbent at equilibrium and the Cr (VI) concentration in solution at equilibrium, respectively. "q_m" (mg/g) is the maximum adsorption capacity exhibited by the adsorbent. "K_L" (L/mg) is the Langmuir constant and is directly related to the energy change of the adsorption process. "K_f" (mg/g $(L/mg)^{1/n}$) and "n" are the Freundlich constants and are related to the adsorption capacity of the adsorbent and the feasibility of the adsorption process, respectively (Nagpal & Kakkar, 2020).

2.9 *Thermodynamics*

To evaluate the effect of temperature on adsorption efficiency, the thermodynamic parameters entropy (ΔS^0), enthalpy (ΔH^0), and Gibbs energy (ΔG^0) (Jiménez-González *et al*., 2024) using equations 8 to 11.

$$\Delta G^0 = \Delta H^0 - T\Delta S^0 \tag{8}$$

$$\Delta G^0 = -RT\ln k_c \tag{9}$$

$$k_c = \frac{q_e}{C_e} \tag{10}$$

$$\ln k_c = -\frac{\Delta H^0}{RT} + \frac{\Delta S^0}{R} \tag{11}$$

Where "T" is the temperature in Kelvin (K), "R" is the universal gas constant in J/mol.K, "k_c" is the equilibrium constant in L/g.

2.10 *Characterization*

Analysis by Attenuated Total Reflectance Fourier-Transform Infrared (ATR-FTIR) of AWP before and after removal of Cr (VI) was realized. This analysis was carried out on the Agilent Cary 630 FTIR spectrometer. A scanning electron microscopy (SEM) analysis was performed to evaluate the morphology of the AWP.

3 Results and discussion

3.1 *Analysis of the experimental design*

Table 2 shows the results corresponding to the removal percentages of the experiments of the 3^2x3 experimental design where the effect of the artichoke residue powder dosage and initial Cr (VI) concentration on the adsorption efficiency determined by the removal percentage is evaluated. The results in this table correspond to the experiments carried out at pH=3, a stirring speed of 150 rpm for 30 minutes, and a temperature of 20 °C.

Table 2. Removal percentages of the experiments of the 3^2x3 experimental design.

Run	Coded factors		Real Factors		Removal (%)
	A	B	A: Dosage of artichoke waste powder (g/L)	B: Initial concentration of Cr (VI) (mg/L)	
1	-1	+1	5	50	50.00
2	0	+1	10	50	48.94
3	0	-1	10	10	45.00
4	-1	-1	5	10	66.67
5	+1	0	15	30	37.21
6	0	0	10	30	47.09
7	-1	0	5	30	55.23
8	+1	+1	15	50	41.84
9	+1	-1	15	10	35.00
10	+1	+1	15	50	36.43
11	0	-1	10	10	44.07
12	-1	-1	5	10	59.32
13	+1	0	15	30	31.95
14	0	0	10	30	51.48
15	0	+1	10	50	51.07
16	+1	-1	15	10	35.59
17	-1	0	5	30	53.85
18	-1	+1	5	50	51.07
19	0	-1	10	10	47.76
20	0	+1	10	50	68.98
21	0	0	10	30	51.48
22	+1	0	15	30	15.82
23	+1	-1	15	10	33.90
24	-1	-1	5	10	61.02
25	-1	0	5	30	51.48
26	+1	+1	15	50	40.00
27	-1	+1	5	50	48.51

Table 3. Analysis of variance of the 3^2x3 experimental design.

Source	**Sum of Squares**	**df**	**Mean Square**	**F-value**	*p-value*
A: Dosage of artichoke waste powder (g/L)	1993.12	1	1993.12	45.35	0.0000
B: Initial concentration of Cr (VI) (mg/L)	4.02	1	4.02	0.09	0.7655
A^2	211.42	1	211.42	4.81	0.0409
AB	218.54	1	218.54	4.97	0.0380
B^2	101.38	1	101.38	2.31	0.1453
Blocks	16.22	2	8.11	0.18	0.8329
Pure Error	835.05	19	43.95		
Cor Total	3379.76	26			

Table 4. Theoretical and practical removal percentage at optimum conditions.

Factor	Optime	Removal (%)	
		Theoretical value	Practical
A: Dosage of artichoke waste powder (g/L)	5.0	60.40	63.37 ± 1.12
B: Initial concentration of Cr (VI) (mg/L)	10.0		

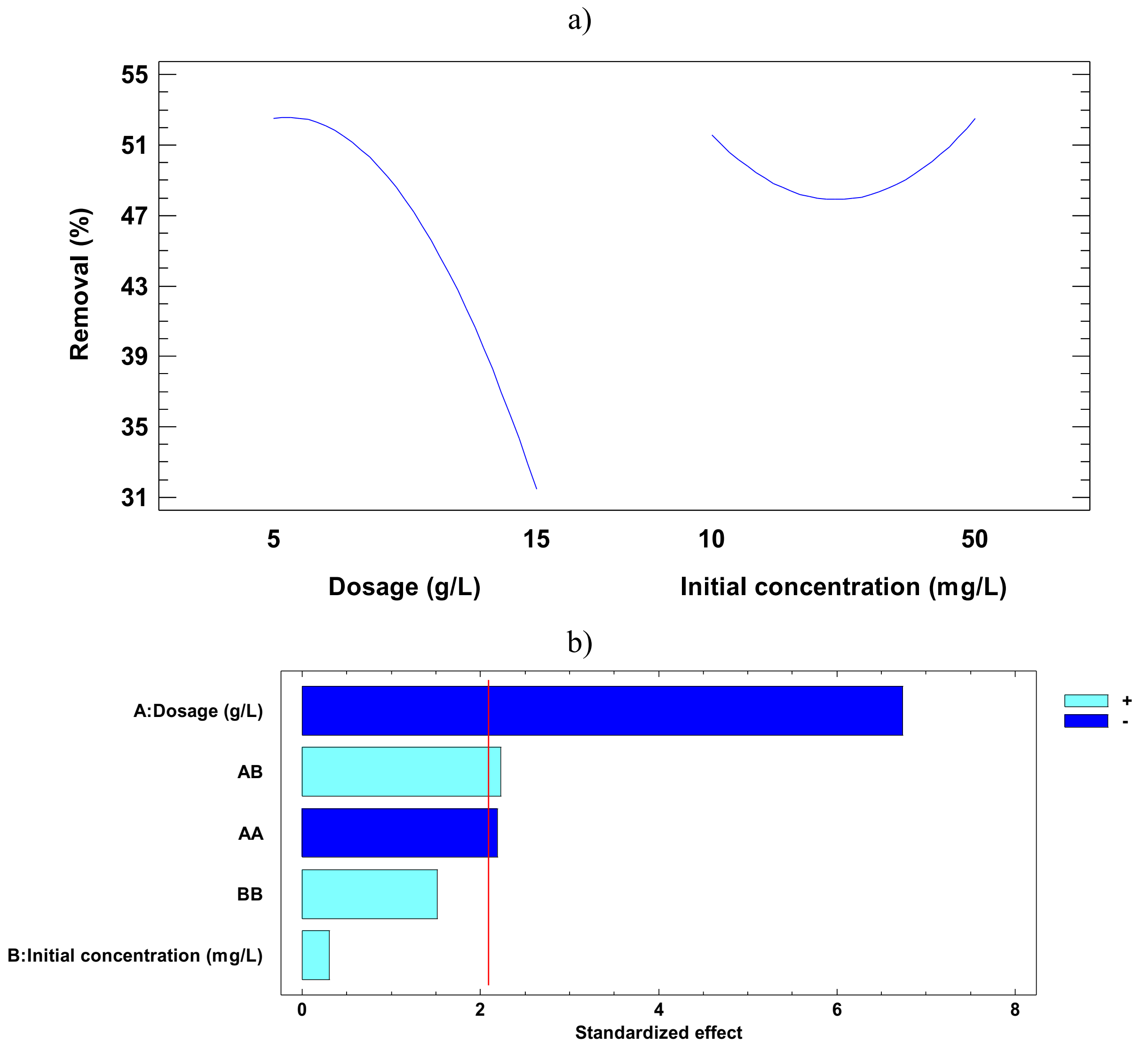

Figure 2. a) Main effects plot and b) standardized Pareto plot for Cr (VI) removal at different artichoke residue powder dosages and initial Cr (VI) concentrations.

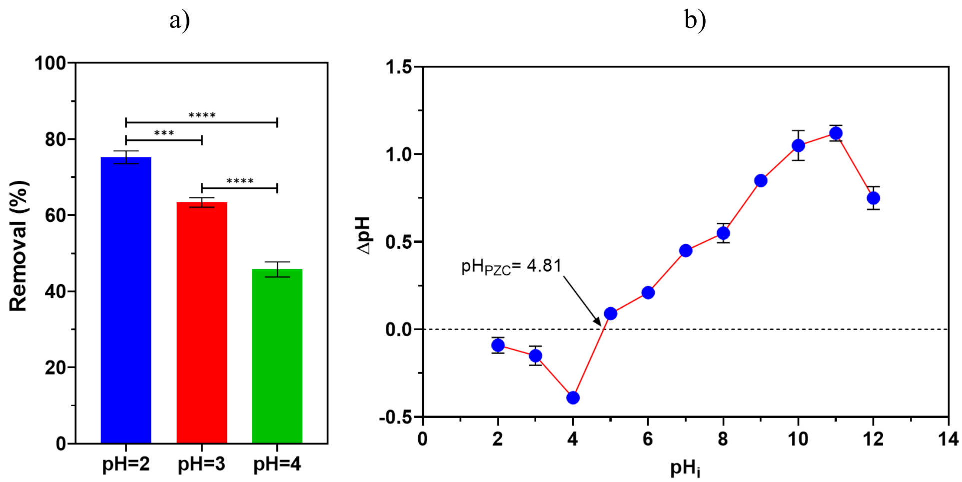

Figure 3. a) Comparison graph of Cr (VI) removal percentages at different pH (Significant difference: ****p<0.0001, ***p<0.001). b) Point of zero charge of artichoke residues.

The analysis of variance of the 3^2x3 design is presented in Table 3. In this statistical analysis, it is shown that the dosage of artichoke residue powder significantly influences the percentage of removal ($p<0.05$), in the same way as its quadratic interaction (A^2) and its interaction with the initial concentration (AB). In contrast, the initial concentration at the conditions proposed in this study does not seem to significantly affect the removal process ($p>0.05$).

The above can be reinforced with Figure 2a, which shows the main effects graph of the Cr (VI) removal percentage. With this figure, it could be said that at a lower dosage, a higher percentage of removal is achieved. As for the Cr (VI) concentration, the lower (10 mg/L) and higher (50 mg/L) concentrations would result in the highest removal percentages. This is confirmed by the Pareto diagram presented in Figure 2b, where it can be seen that the artichoke powder dosage achieves a negative result in the percentage of removal, since as the dosage increases, lower removal percentages are obtained, and it can also be seen that the most significant factor is the adsorbent dosage.

This is because at very high adsorbent dosages the adsorption capacity may show a decreasing trend due to aggregation and overlapping of active sites leading to a decrease in surface area and a lower rate of diffusion of metal ions into the adsorbent matrix (Bencheikh *et al*., 2021).

On the other hand, equation 12 presents the mathematical model of the experimental design that serves to make theoretical predictions of the removal percentage (%*R*) where "*A*" is the artichoke powder dosage and "*B*" is the initial concentration of Cr (VI)

$$\%R = 66.55 + 1.36A - 1.02B - 0.24A^2 + 0.043AB + 0.0103B^2 \quad (12)$$

With the above model, the Statgraphics Centurion software allowed the optimization analysis of the adsorption process (Table 4) studied achieving a theoretical maximum removal rate of 60.40% which is achieved at an initial Cr (VI) concentration of 10 mg/L and 5 g/L dosage of artichoke residue powder. Table 4 shows the results of the practical analysis carried out in the laboratory at optimum conditions of the model, achieving a removal percentage of 63.37 ± 1.12 %, which is similar to the theoretical value predicted by the model.

3.2 Effect of pH on the removal process

To evaluate the pH of the removal process, Cr (VI) removal experiments were carried out at pH values of 2, 3, and 4. These experiments were performed at the optimum conditions of Table 4. Figure 3a shows the results, where it is observed that at pH=2 75.24 ± 1.68 % was removed, at pH=3 63.37 ± 1.12 % was removed, and at pH=4 a removal of 45.78 ± 1.9 % was achieved. This figure also shows the analysis of the variance of the removal percentages obtained, showing that at pH=2, significantly higher removal percentages were achieved than at pH values of 3 and 4. In this respect, Cr (VI) adsorption is favored at acidic pH (high H^+ concentration) due to the protonation of the adsorbent medium (Fenti *et al*., 2020). This is corroborated by looking at Figure 3b where it is observed that the point of zero charge of the artichoke powder is pH_{PZC}= 4.81, this indicates that at pH=4.81 the charge of the adsorbent is zero, therefore, at a higher pH where there is a higher concentration of OH^- the artichoke powder would be negatively charged, on the contrary, at lower pH where there is a higher concentration of H^+ it would be positively charged. This would explain that at lower pH higher removal percentages are achieved since the artichoke powder, being positively charged, has a higher pH (Saavedra *et al*., 2019), and Cr (VI) as dichromate anion would be adsorbed by electrostatic attraction.

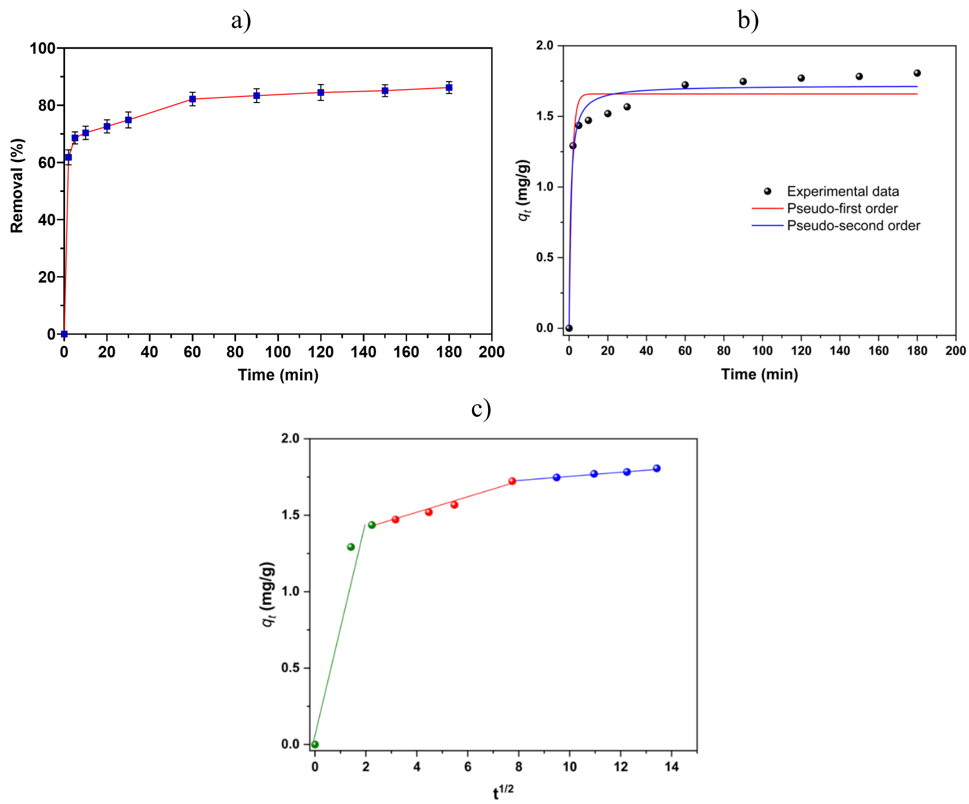

Figure 4. a) Percentage Cr (VI) removal as a function of time. b) Pseudo-first order kinetics (red line) and pseudo-second order kinetics (blue line), and c) intraparticle diffusion model.

3.3 Adsorption kinetics of Cr (VI)

For the kinetic study, the agitation time was extended to 180 minutes, the conditions being pH=2, a dosage of 5 g/L of artichoke residue powder, and an initial Cr (VI) concentration of 10 mg/L at 150 rpm. Figure 4a shows the results of the removal percentage as a function of time, showing that the highest Cr (VI) adsorption occurs in the first minutes. This is because at the beginning of the adsorption process, the attraction between the adsorbate and the adsorbent is greater, since all the surface is available, as this phenomenon takes place, the free available surface decreases, so the removal percentage tends to become constant (Afroze & Sen, 2018).

Subsequently, the kinetic fit of the pseudo-first-order and pseudo-second-order kinetic models to the removal process was evaluated. Figure 4b shows the results, where it is graphically observed that the pseudo-second order model is a better fit to the experimental data than the pseudo-first order model. The parameter values of both kinetic models are presented in Table 5. It is observed that the pseudo-second order kinetic model fits the experimental data better with an R^2 of 0.9706 which is higher than the R^2 of the pseudo-first order model (R^2=0.9348). The pseudo-second order model provides the parameters "q_e" corresponding to the extent of the adsorption process and "k_2", to the rate of the adsorption process. On the other hand, the pseudo-second order model indicates that the adsorption process corresponds to chemical adsorption (Jamil *et al*., 2023).

Figure 4c shows the linear graph of the intraparticle diffusion model, where three different linear regions (three stages) are presented, which would indicate that the adsorption of Cr (VI) on artichoke residue powder involves more than one kinetic mechanism. (Xu *et al*., 2019). The first stage would occur in the first five minutes where surface diffusion would be taking place, which translates into a surface adsorption controlled by the diffusion of the boundary layer. From 5 to 60 minutes, the second stage, which corresponds to intraparticle diffusion, is presented, with a decrease in the adsorption rate. This indicates that intraparticle diffusion was the limiting mechanism for the Cr (VI) adsorption rate on artichoke powder. Finally, the third stage would correspond to the adsorption equilibrium where there is a decrease in the concentration of Cr (VI) in the solution which makes the diffusion rate decrease further achieving the adsorption equilibrium. Table 5 shows the values of the intra-particle diffusion parameters calculated according to (Wang *et al*., 2025), where it is observed that the reaction rate constant $K_{id,1}$ is greater than $K_{id,2}$ which would indicate that in the first stage, all Cr (VI) binding sites are occupied, thus increasing the

Table 5. Parameter values of the pseudo-first order and pseudo-second order kinetic models.

Model		Parameter	Value
		q_{exp} (mg/g)	1.75
Pseudo first order		k_1 (min^{-1})	0.680
		$q_{e, cal}$ (mg/g)	1.66
		R^2	0.9348
Pesudo second order		k_2 ($g\ mg^{-1} min^{-1}$)	0.682
		$q_{e, cal}$ (mg/g)	1.72
		R^2	0.9706
Intraparticle diffusion	First stage	$K_{id,1}$ ($mg/g{\cdot}min^{1/2}$)	0.672
		C_1	0.092
		R^2	0.9231
	Second stage	$K_{id,2}$ ($mg/g{\cdot}min^{1/2}$)	0.056
		C_2	1.280
		R^2	0.9782
	Third stage	$K_{id,3}$ ($mg/g{\cdot}min^{1/2}$)	0.015
		C_3	1.608
		R^2	0.9831

q_{exp}: Experimental adsorption capacity

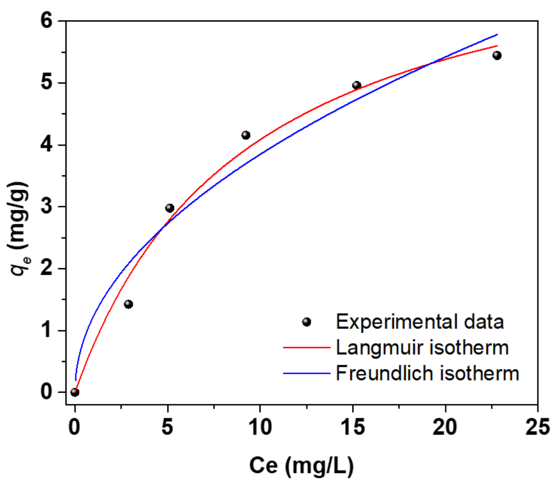

Figure 5. Graph of adsorption isotherms. Langmuir isotherm (red line) and Freundlich isotherm (blue line).

diffusion resistance of Cr (VI). On the other hand, Table 5 also presents the values of the boundary layer coefficients (C) corresponding to the thickness of the boundary layer where C_1 is the surface diffusion boundary layer and C_2 is the internal diffusion layer. The higher C_2 than C_1 confirms that adsorption would be mainly influenced by intraparticle diffusion (Wang *et al.*, 2025), however, other mechanisms would be involved because C is different from zero (Jasper *et al.*, 2020), which would indicate that the process would also be controlled by diffusion in the boundary layer (Agbor Tabi *et al.*, 2022).

3.4 Adsorption isotherms of Cr (VI)

Figure 5 shows the fit plot to the mathematical models of the Langmuir and Freundlich adsorption isotherms.

Table 6. Parameter values of the Langmuir and Freundlich isotherm models.

Model	Parameters	Value
Langmuir	q_m (mg/g)	7.89
	K_L *(L/mg)*	0.107
	R^2	0.9827
Freundlich	*1/n*	0.495
	K_f ($mg/g\ (L/mg)^{1/n}$)	1.231
	R^2	0.8917

A better fit of the data to the Langmuir isotherm is graphically observed. Table 6 presents the parameters of both isotherm models where it is observed that the Langmuir isotherm fits better to the adsorption process of Cr (VI) by artichoke residue powder with an R^2 of 0.9827 which is higher than the R^2 of the Freundlich isotherm (R^2=0.8917). This indicates that the main Cr (VI) adsorption process corresponds to monolayer adsorption (Fernández-López *et al.*, 2019). The adsorption capacity "q_m" of artichoke powder in tea filter bags is 7.89 mg/g.

Table 7 shows the adsorption capacities of different natural adsorbents where Artichoke waste shows the highest adsorption capacity.

3.5 Thermodynamics of Cr (VI) adsorption process

The thermodynamic parameters of the adsorption process are presented in Table 8. The entropy ΔS^0 has a value of 242.11 J/mol.K. The positive value of ΔS^0 illustrates increased randomness at the solid/liquid interface during Cr (VI) adsorption (Jamil *et al.*, 2023) on artichoke waste powder. The enthalpy ΔH^0 has a value of 70.84 kJ/mol.

Table 7. Maximum adsorption capacity of Cr (VI) of different natural adsorbents.

Adsorbent	q_m (mg/g)	Reference
Orange peel	1.90	(López-Téllez et al., 2011)
Soy hull biomass	7.286	(Blanes et al., 2016)
Tea and ginger	7.29	(Sharma et al., 2016)
Magnolia leaf	3.96	(Mondal et al., 2019)
Cranberry kernel shell	6.81	(Parlayici & Pehlivan, 2019)
Functionalized peanut shells	5.36	(Li et al., 2022)
Sesbania sesban biochar	5.3	(Vu et al., 2024)
Artichoke waste	7.89	This research

Table 8. Values of thermodynamic parameters of the adsorption process.

T(K)	ΔS^0 (J/mol.K)	ΔH^0 (kJ/mol)	ΔG^0 (kJ/mol)
293	242.11	70.84	-0.55
303			-1.55
313			-5.46

The positive value of ΔH^0 indicates that the adsorption process is endothermic, in addition, the value of ΔH^0 found shows that the process corresponds to chemical adsorption being within the range of 20.9-418.4 kJ/mol (Jamil *et al.*, 2023). Finally, the Gibbs energy ΔG^0 becomes more negative as the temperature increases. The negative value of ΔG^0 (-0.55, -1.55, y -5.46 kJ/mol) indicates that the process is spontaneous.

3.6 Characterization of artichoke residue powder

Fourier transform infrared spectroscopy (FTIR) analysis was performed to know the nature of the functional groups that could be present in the adsorbent. The FTIR spectra of the artichoke residue powder before adsorption are presented in Figure 6 (black line). It is observed that 3314.5 cm^{-1} presents a stretching vibration of the -O-H groups. At 2916.3 and 2949.3 cm^{-1} corresponding to the stretching vibrations of the $-CH_3$ groups. At 1741.1 cm^{-1} there are stretching vibrations of C=O. Also, there are stretching vibrations from 758 to 1606.4 cm^{-1} that could correspond to the aromatic groups of the compounds present in the adsorbent. The FTIR spectra after adsorption of Cr (VI) on the artichoke residue powder are presented in Figure 6 (red line), where it is observed that changes are presented compared to the spectra in Figure 6 specifically at 3314.5, 2916.3, 2949.3, 1741.1, and 758 cm^{-1}. These findings are in agreement with the current literature since apparently, the artichoke residue powder would present carboxyl groups and aromatic rings characteristic of lignocellulosic compounds (Saavedra *et al.*, 2019).

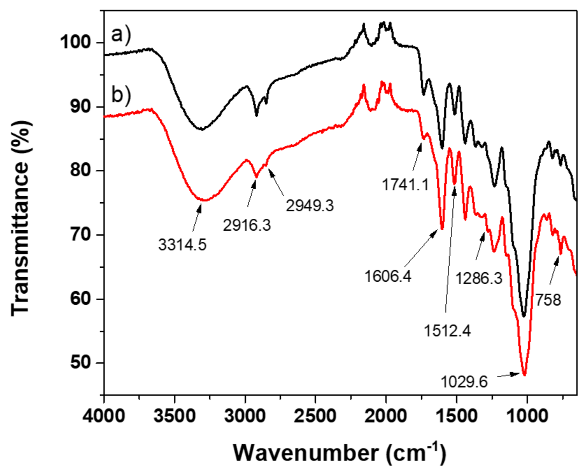

Figure 6. FTIR spectra of artichoke residues a) before adsorption (black line) and b) after adsorption (red line) of Cr (VI).

Figure 7 presents the micrographs obtained by SEM of the artichoke residue powder. Figure 9a presents a micrograph where the particles of the adsorbent are shown in comparison with a scale of 100 μm at 1000x and Figure 9b in comparison with a scale of 10 μm at 10000x. It is observed that the adsorbent presents irregularities in its surface having a structure of smooth parts and with cavities. This type of rough surface would facilitate the adsorption or fixation of heavy metals (Saavedra *et al.*, 2019).

Conclusions

In the present research, the removal of Cr (VI) from water in a batch agitation system using artichoke waste powder packed in filter bags was evaluated.

a) b)

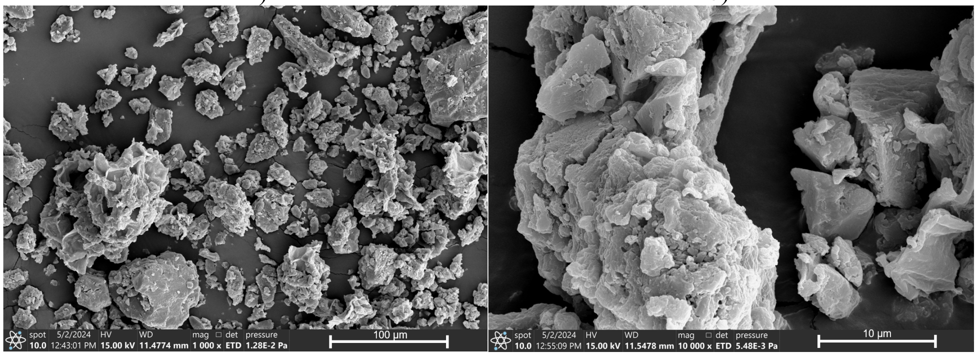

Figure 7. SEM microphotographs of artichoke surface at a) 1000x, and b) 10000x.

The adsorbent dosage and pH were found to be the most important factors that significantly affected the adsorption efficiency. FTIR analysis of artichoke powder showed the presence of hydroxyl, carbonyl, aromatic, and hydrocarbon chain groups characteristic of the lignocellulosic compounds involved in the adsorption process. SEM micrographs show that this residue presents an irregular and rough structure where Cr (VI) is being adsorbed. The adsorption process was more accurately described using the pseudo-second order kinetic model (R^2=0.9969). Analysis of the adsorption isotherm according to the Langmuir model (R^2=0.9827) indicates that Cr (VI) removal occurs by monolayer adsorption. The maximum adsorption capacity was 7.89 mg/g. The evaluation of the thermodynamic parameters indicates that the adsorption process of Cr (VI) on artichoke powder is endothermic and spontaneous. In conclusion, the Cr (VI) removal process using artichoke powder in filter bags corresponds to an effective, simple, low-cost, and environmentally friendly process.

Acknowledgments

The authors would like to thank the Universidad Tecnológica del Perú for financing this research under the code "I+D_SUR_2021_017".

References

Afroze, S., & Sen, T. K. (2018). A Review on Heavy Metal Ions and Dye Adsorption from Water by Agricultural Solid Waste Adsorbents. *Water, Air, & Soil Pollution*, *229*(7), 225. https://doi.org/10.1007/s11270-018-3869-z

Agbor Tabi, G., Ngouateu Rene Blaise, L., Daouda, K., Naphtali Odogu, A., Aime Victoire, A., Nsami Julius, N., & Joseph Mbadcam, K. (2022). Non-linear modelling of the adsorption of Indigo Carmine dye from wastewater onto characterized activated carbon/volcanic ash composite. *Arabian Journal of Chemistry*, *15*(1), 103515. https://doi.org/10.1016/j.arabjc.2021.103515

Ali, H., Khan, E., & Ilahi, I. (2019). Environmental Chemistry and Ecotoxicology of Hazardous Heavy Metals: Environmental Persistence, Toxicity, and Bioaccumulation. *Journal of Chemistry*, *2019*, e6730305. https://doi.org/10.1155/2019/6730305

Arief, V. O., Trilestari, K., Sunarso, J., Indraswati, N., & Ismadji, S. (2008). Recent Progress on Biosorption of Heavy Metals from Liquids Using Low Cost Biosorbents: Characterization, Biosorption Parameters and Mechanism Studies. *CLEAN – Soil, Air, Water*, *36*(12), 937–962. https://doi.org/10.1002/clen.200800167

Arshad, F., Selvaraj, M., Zain, J., Banat, F., & Haija, M. A. (2019). Polyethylenimine modified graphene oxide hydrogel composite as an efficient adsorbent for heavy metal ions. *Separation and Purification Technology*, *209*, 870–880. https://doi.org/10.1016/j.seppur.2018.06.035

Bencheikh, I., Azoulay, K., Mabrouki, J., El Hajjaji, S., Dahchour, A., Moufti, A., & Dhiba, D. (2020). The adsorptive removal of MB using chemically treated artichoke leaves: Parametric, kinetic, isotherm and thermodynamic study. *Scientific African*, *9*, e00509. https://doi.org/10.1016/j.sciaf.2020.e00509

Bencheikh, I., Azoulay, K., Mabrouki, J., El Hajjaji, S., Moufti, A., & Labjar, N. (2021). The use and the performance of chemically treated artichoke leaves for textile industrial effluents treatment. *Chemical Data Collections*, *31*, 100597. https://doi.org/10.1016/j.cdc.2020.100597

Blanes, P. S., Bordoni, M. E., González, J. C., García, S. I., Atria, A. M., Sala, L. F., & Bellú, S. E. (2016). Application of soy hull biomass in removal of Cr(VI) from contaminated waters. Kinetic, thermodynamic and continuous sorption studies. *Journal of Environmental Chemical Engineering*, *4*(1), 516–526. https://doi.org/10.1016/j.jece.2015.12.008

Choquenaira-Quispe, C., Villanueva-Salas, J. A., Yucra-Condori, H. R., Angulo Vargas, S. J., Rojas Tamata, K., & Gonzales-Condori, E. G. (2024). "Chacco" clay from the Peruvian highlands as a potential adsorbent of heavy metals in water. *Energy Nexus*, *16*, 100330. https://doi.org/10.1016/j.nexus.2024.100330

de Diego-Díaz, B., Peñas, F. J., & Fernández-Rodríguez, J. (2021). Sustainable management of lignocellulosic wastes: Temperature strategies for anaerobic digestion of artichoke. *Journal of Cleaner Production*, *280*, 124479. https://doi.org/10.1016/j.jclepro.2020.124479

Dobrowolski, R., Krzyszczak, A., Dobrzyńska, J., Podkościelna, B., Zięba, E., Czemierska, M., Jarosz-Wilkołazka, A., & Stefaniak, E. A. (2019). Extracellular polymeric substances immobilized on microspheres for removal of heavy metals from aqueous environment. *Biochemical Engineering Journal*, *143*, 202–211. https://doi.org/10.1016/j.bej.2019.01.004

Elgarahy, A. M., Elwakeel, K. Z., Mohammad, S. H., & Elshoubaky, G. A. (2021). A critical review of biosorption of dyes, heavy metals and metalloids from wastewater as an efficient and green process. *Cleaner Engineering and Technology*, *4*, 100209. https://doi.org/10.1016/j.clet.2021.100209

Ergüvenerler, F., Targan, Ş., & Tirtom, V. N. (2020). Removal of lead from aqueous solutions by low cost and waste biosorbents (lemon, bean and artichoke shells). *Water Science and Technology*, *81*(1), 159–169. https://doi.org/10.2166/wst.2020.093

FAO. (2018). *Estadísticas | Food and Agriculture Organization (FAO) | Organización de las Naciones Unidas para la Alimentación y la Agricultura*. https://www.fao.org/statistics/es

Fenti, A., Chianese, S., Iovino, P., Musmarra, D., & Salvestrini, S. (2020). Cr(VI) Sorption from Aqueous Solution: A Review. *Applied Sciences*, *10*(18), Article 18. https://doi.org/10.3390/app10186477

Fernández-López, J. A., Angosto, J. M., Roca, M. J., & Doval Miñarro, M. (2019). Taguchi design-based enhancement of heavy metals bioremoval by agroindustrial waste biomass from artichoke. *Science of The Total Environment*, *653*, 55–63. https://doi.org/10.1016/j.scitotenv.2018.10.343

Fouda, A., Hassan, S. E.-D., Abdel-Rahman, M. A., Farag, M. M. S., Shehal-deen, A., Mohamed, A. A., Alsharif, S. M., Saied, E., Moghanim, S. A., & Azab, M. S. (2021). Catalytic degradation of wastewater from the textile and tannery industries by green synthesized hematite (α-Fe2O3) and magnesium oxide (MgO) nanoparticles. *Current Research in Biotechnology*, *3*, 29–41. https://doi.org/10.1016/j.crbiot.2021.01.004

Gonzales-Condori, E., Avalos-López, G., Mujica-Guzman, A., Terán-Hilares, R., Briceño, G., Quispe-Avilés, J., Parra, P., & Villanueva-Salas, J. (2023). Avocado seed powder residues as a promising bio-adsorbent for color removal from textile wastewater. *Revista Mexicana de Ingeniería Química*, *22*. https://doi.org/10.24275/rmiq/IA2370

Hajji Nabih, M., El Hajam, M., Boulika, H., Chiki, Z., Ben Tahar, S., Idrissi Kandri, N., & Zerouale, A. (2023). Preparation and characterization of activated carbons from cardoon "*Cynara Cardunculus*" waste: Application to the adsorption of synthetic organic dyes. *Materials Today: Proceedings*, *72*, 3369–3379. https://doi.org/10.1016/j.matpr.2022.07.414

Hossain, K. F. B., Sikder, Md. T., Rahman, Md. M., Uddin, Md. K., & Kurasaki, M. (2017). Investigation of Chromium Removal Efficacy from Tannery Effluent by Synthesized Chitosan from Crab Shell. *Arabian Journal for Science and Engineering*, *42*(4), 1569–1577. https://doi.org/10.1007/s13369-017-2435-0

Jamil, U., Zeeshan, M., Khan, S. R., & Saeed, S. (2023). Synthesis and two-step KOH based activation of porous biochar of wheat straw and waste tire for adsorptive exclusion of chromium (VI) from aqueous solution; thermodynamic and regeneration study. *Journal of Water Process Engineering*, *53*, 103892. https://doi.org/10.1016/j.jwpe.2023.103892

Jasper, E. E., Ajibola, V. O., & Onwuka, J. C. (2020). Nonlinear regression analysis of the sorption of crystal violet and methylene blue from aqueous solutions onto an agro-waste derived activated carbon. *Applied Water Science*, *10*(6), 132. https://doi.org/10.1007/s13201-020-01218-y

Jiménez-González, A., Tec-Caamal, E. N., Medina-Moreno, S. A., & Universidad Politécnica de Pachuca. (2024). Biosorption performance evaluation of azo dyes Reactive Red 2 and Reactive Blue 4 on thermally sterilized biomass of Cladosporium tenuissimum fungus. *Revista Mexicana de Ingeniería Química*, *23*(1), 1–33. https://doi.org/10.24275/rmiq/IA24161

Khalfaoui, A., Benalia, A., Laggoun, Z., Bouchareb, R., Zaamta, I., Melloul, R., Menasria, A., Merouani, S., Pizzi, A., & Derbal, K. (2024). Effective synthesis and application of artichoke and orange peels-based bio-sorbents for Ketoprofen removal from wastewater: Process optimization using Factorial methodology. *Desalination and Water Treatment*, *317*, 100197. https://doi.org/10.1016/j.dwt.2024.100197

Khalfaoui, A., Khelifi, M. N., Khelfaoui, A., Benalia, A., Derbal, K., Gisonni, C., Crispino, G., & Panico, A. (2022). The Adsorptive Removal of Bengal Rose by Artichoke Leaves: Optimization by Full Factorials Design. *Water*, *14*(14), Article 14. https://doi.org/10.3390/w14142251

Lattanzio, V., Kroon, P. A., Linsalata, V., & Cardinali, A. (2009). Globe artichoke: A functional food and source of nutraceutical ingredients. *Journal of Functional Foods*, *1*(2), 131–144. https://doi.org/10.1016/j.jff.2009.01.002

Li, Q., Huang, Q., Pan, X. Y., Yu, H., & Zhao, Z. T. (2022). Adsorption behavior of Cr(VI) by biomass-based adsorbent functionalized with deep eutectic solvents (DESs). *BMC Chemistry*, *16*(1), 41. https://doi.org/10.1186/s13065-022-00834-w

López-Téllez, G., Barrera-Díaz, C. E., Balderas-Hernández, P., Roa-Morales, G., & Bilyeu, B. (2011). Removal of hexavalent chromium in aquatic solutions by iron nanoparticles embedded in orange peel pith. *Chemical Engineering Journal*, *173*(2), 480–485. https://doi.org/10.1016/j.cej.2011.08.018

Mondal, N. K., Samanta, A., Roy, P., & Das, B. (2019). Optimization study of adsorption parameters for removal of Cr(VI) using Magnolia leaf biomass by response surface methodology. *Sustainable Water Resources Management*, *5*(4), 1627–1639. https://doi.org/10.1007/s40899-019-00322-5

Nagpal, M., & Kakkar, R. (2020). Facile synthesis of mesoporous magnesium oxide–graphene oxide composite for efficient and highly selective adsorption of hazardous anionic dyes. *Research on Chemical Intermediates*, *46*(5), 2497–2521. https://doi.org/10.1007/s11164-020-04103-0

Parlayici, Ş., & Pehlivan, E. (2019). Comparative study of Cr(VI) removal by bio-waste adsorbents: Equilibrium, kinetics, and thermodynamic. *Journal of Analytical Science and Technology*, *10*(1), 15. https://doi.org/10.1186/s40543-019-0175-3

Petrella, A., Spasiano, D., Rizzi, V., Cosma, P., Race, M., & De Vietro, N. (2018). Lead Ion Sorption by Perlite and Reuse of the Exhausted Material in the Construction Field. *Applied Sciences*, *8*(10), Article 10. https://doi.org/10.3390/app8101882

Quattrocchi, O., Abelaira, S., & Felipe Laba, R. (1992). *Introduccion a la HPLC, Aplicacion y Practica*.

Que, W., Zhou, Y., Liu, Y., Wen, J., Tan, X., Liu, S., & Jiang, L. (2019). Appraising the effect of in-situ remediation of heavy metal contaminated sediment by biochar and activated carbon on Cu immobilization and microbial community. *Ecological Engineering*, *127*, 519–526. https://doi.org/10.1016/j.ecoleng.2018.10.005

Rambabu, K., Bharath, G., Banat, F., & Show, P. L. (2020). Biosorption performance of date palm empty fruit bunch wastes for toxic hexavalent chromium removal. *Environmental Research*, *187*, 109694. https://doi.org/10.1016/j.envres.2020.109694

Rosique, M., Angosto, J. M., Guibal, E., Roca, M. J., & Fernández-López, J. A. (2016). Factorial Design Methodological Approach for Enhanced Cadmium Ions Bioremoval by Opuntia Biomass. *CLEAN – Soil, Air, Water*, *44*(8), 959–966. https://doi.org/10.1002/clen.201500368

Saavedra, M. I., Doval Miñarro, M., Angosto, J. M., & Fernández-López, J. A. (2019). Reuse potential of residues of artichoke (*Cynara scolymus* L.) from industrial canning processing as sorbent of heavy metals in multimetallic effluents. *Industrial Crops and Products*, *141*, 111751. https://doi.org/10.1016/j.indcrop.2019.111751

Salazar-Pinto, B. M., Zea-Linares, V., Villanueva-Salas, J. A., & Gonzales-Condori, E. G. (2021). Cd (II) and Pb (II) biosorption in aqueous solutions using agricultural residues of Phaseolus vulgaris L.: Optimization, kinetics, isotherms and desorption. *Revista Mexicana de Ingeniería Química*, *20*(1), Article 1. https://doi.org/10.24275/rmiq/IA1864

Samghouli, N., Bencheikh, I., Azoulay, K., Abahdou, F.-Z., Mabrouki, J., & El Hajjaji, S. (2022). Study of Piroxicam Removal from Wastewater by Artichoke Waste Using NemrodW® Software: Statistical Analysis. In M. Azrour, A. Irshad, & R. Chaganti (Eds.), *IoT and Smart Devices for Sustainable Environment* (pp. 29–42). Springer International Publishing. https://doi.org/10.1007/978-3-030-90083-0_3

Sharma, P. K., Ayub, S., & Tripathi, C. N. (2016). Isotherms describing physical adsorption of Cr(VI) from aqueous solution using various agricultural wastes as adsorbents. *Cogent Engineering*, *3*(1), 1186857. https://doi.org/10.1080/23311916.2016.1186857

Sun, S., Zhu, J., Zheng, Z., Li, J., & Gan, M. (2019). Biosynthesis of β-cyclodextrin modified Schwertmannite and the application in heavy metals adsorption. *Powder Technology*, *342*, 181–192. https://doi.org/10.1016/j.powtec.2018.09.072

Vu, T. P., Quyen, L. T. T., Hiep, N. T., Thu, T. T. H., & Suong, T. T. (2024). Hexavalent Chromium Adsorption on Adsorbent Derived From Biomass of Fabaceae Plant in Vietnam: Effect of Preparation Conditions on Equilibrium Adsorption Capacity. *Environmental Quality Management*, *34*(2), e22353. https://doi.org/10.1002/tqem.22353

Wang, W., Wei, P., Wang, C., Liang, P., Tao, F., Yang, S., Dou, W., & Hu, B. (2025). Honeycomb-structured biochar from waste pomelo peel for synergistic adsorptive and photocatalytic removal of Cr(VI). *Carbon Research*, *4*(1), 10. https://doi.org/10.1007/s44246-024-00174-5

Worku, Z., Tibebu, S., Nure, J. F., Tibebu, S., Moyo, W., Ambaye, A. D., & Nkambule, T. T. I. (2023). Adsorption of chromium from electroplating wastewater using activated carbon developed from water hyacinth. *BMC Chemistry*, *17*(1), 85. https://doi.org/10.1186/s13065-023-00993-4

Xu, Y., Chen, J., Chen, R., Yu, P., Guo, S., & Wang, X. (2019). Adsorption and reduction of chromium(VI) from aqueous solution using polypyrrole/calcium rectorite composite adsorbent. *Water Research*, *160*, 148–157. https://doi.org/10.1016/j.watres.2019.05.055

Yang, J., Huang, B., & Lin, M. (2020). Adsorption of Hexavalent Chromium from Aqueous Solution by a Chitosan/Bentonite Composite: Isotherm, Kinetics, and Thermodynamics Studies. *Journal of Chemical & Engineering Data*, *65*(5), 2751–2763. https://doi.org/10.1021/acs.jced.0c00085

Zhang, X., Cui, L., Chen, B., Xiong, Q., Zhan, Y., Ye, J., & Yin, Q. (2021). Effect of chromium supplementation on hs-CRP, TNF-α and IL-6 as risk factor for cardiovascular diseases: A meta-analysis of randomized-controlled trials. *Complementary Therapies in Clinical Practice*, *42*, 101291. https://doi.org/10.1016/j.ctcp.2020.101291

Zhao, M., Xu, Y., Zhang, C., Rong, H., & Zeng, G. (2016). New trends in removing heavy metals from wastewater. *Applied Microbiology and Biotechnology*, *100*(15), 6509–6518. https://doi.org/10.1007/s00253-016-7646-x

Zuorro, A., Maffei, G., & Lavecchia, R. (2016). Reuse potential of artichoke (Cynara scolimus L.) waste for the recovery of phenolic compounds and bioenergy. *Journal of Cleaner Production*, *111*, 279–284. https://doi.org/10.1016/j.jclepro.2015.06.011